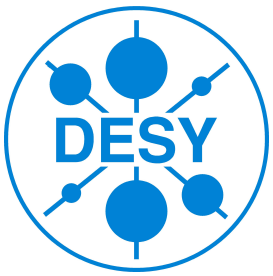

Diffractive dissociation cross sections in pp collisions at $\sqrt{s} = 7$ TeV

Juan Leopoldo Cuspinera Contreras

Deutsches Elektronen Synchrotron, Hamburg, Germany

Abstract: Results of different PYTHIA tunings are compared to the CMS measurements of the diffractive dissociation cross sections in pp collisions at $\sqrt{s} = 7$ TeV. The definition of the hadron level to which the data are corrected is based on [1]. Differential cross sections are obtained as a function of $\xi_X = M_X^2/s$ in the region $-5.5 < \log_{10}\xi_X < -2.5$, for $\log_{10}(M_Y/\text{GeV}) < 0.5$, dominated by single diffractive dissociation (SD), and $0.5 < \log_{10}(M_Y/\text{GeV}) < 1.1$, dominated by double diffractive dissociation (DD), where M_X and M_Y are the masses of the two final-state hadronic systems separated by the largest rapidity gap in an event. The cross section is also measured as a function of the width of the central rapidity gap $\Delta\eta$ for $\Delta\eta > 3$, $\log_{10}(M_X/\text{GeV}) > 1.1$ and $\log_{10}(M_Y/\text{GeV}) > 1.1$, dominated by DD.

Contents

1 Introduction **3**

1.1 CMS detector 4

1.2 Monte Carlo generators 4

1.3 Diffractive event topologies 5

2 Forward rapidity gap cross section **6**

3 Central rapidity gap cross section **10**

4 Summary **12**

5 Acknowledgments **13**

1 Introduction

Diffractive interactions provide a significant fraction ($\approx 25\%$) of the total inelastic proton-proton (pp) cross section within the high energies domain. These events are characterized by at least one non-exponentially suppressed large rapidity gap (LRG), *i.e.* a region in pseudorapidity η devoid of particles, where $\eta \equiv -\ln[\tan(\theta/2)]$ and θ is the polar angle of the particle. These kind of LRG are presumed to be obtained by a colour-singlet (colourless) exchange carrying the vacuum quantum numbers, commonly referred to as a Pomeron ($\mathbb{P}$) exchange. Figure 1 shows the types of diffractive processes: SD, DD and CD.

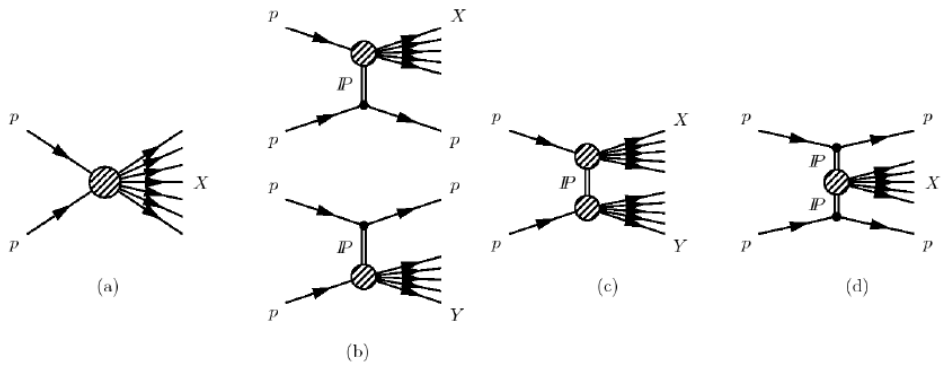

Figure 1: Schematic diagrams of (a) Non Diffractive (ND) process, (b) Single Diffractive dissociation (SD), (c) Double Diffractive dissociation (DD) and (d) Central Diffractice dissociation (CD).

Diffractive processes are described in the framework of Regge theory. Different models based on this theory give different predictions when extrapolated from a center-of-mass energy $\sqrt{s} \leq 1.96$ TeV to the LHC center-of-mass-energy $\sqrt{s} = 7$ TeV. Therefore the measurements of the diffractive cross sections at the LHC provide a valuable input to understand diffraction and to improve the Monte Carlo (MC) event generators.

In this work MC predictions of different PYTHIA tunings are compared to the data obtained in the first measurement of inclusive diffractive cross sections at the Compact Muon Solenoid (CMS) experiment at $\sqrt{s} = 7$ TeV. The measurement is based on the presence of a forward LRG in the event,

and we separate SD- and DD-dominated event samples by using the Centauro And Strange Object Research (CASTOR calorimeter) which covers the forward region $-6.6 < \eta < -5.2$. A data sample with a central LRG, in which DD dominates, is also defined. The measurement was made during the 2010 commissioning period, when the probability of having a pileup in pp collisions was low.

1.1 CMS detector

The CMS experiment uses a right-handed coordinate system, with its origin at the collision point. The x axis points to the center of the LHC, while the y axis points upward relative to the LHC plane, and the z axis is along the anticlockwise beam direction. The polar angle θ is measured from the positive z axis. To assure a reliable Monte Carlo description the two most forward rings of the hadron calorimeter HF are not used and therefore the central CMS detector will cover the region $|\eta| \lesssim 4.7$ while the CASTOR covers the forward region $-6.6 < \eta < -5.2$.

The CASTOR calormeter used to detect a low-mass system escaping the detection in the central CMS detector is only located on the negative η region. The final results for the cross sections are obtained by assuming a symmetry around $\eta = 0$.

1.2 Monte Carlo generators

We compare the diffractive cross sections measurements from [1] to the predictions made by different tunings of Pythia, namely Pythia8-4C [2], ATLAS MB [2], the Monash 2013 tune [3] and the Minimum Bias Rockefeller (MBR) [4] model implemented in Pythia8 (Pythia8 - MBR).

We use the standard configuration for the Pythia8 MBR model in which the Pomeron trajectory $\alpha(t) = 1 + \varepsilon + \alpha' t$ is using the parameter values $\varepsilon = 0.08$ and $\alpha' = .025$ GeV^{-1}, with t the four-momentum transfer squared at the proton vertex.

1.3 Diffractive event topologies

The inclusive inelastic events in the region covered by the central CMS detector are dominated by non-diffractive (ND) events for which final state particle production occurs in the entire η space available. On the other hand diffractive events are expected to have a LRG in the final state. We consider two different topologies (figure 2), depending on the position of the LRG in the central CMS detector:

- FG: a forward rapidity gap at the edge on the negative η side of the detector.
- CG: a central pseudorapidity gap in the detector around $\eta = 0$.

Other topologies, such as the one with a gap on each edge of the detector, are neglected because of the limited number of such events. For the FG topology the pseudorapidity gap is related to the η_{min} variable defined as the lowest η, respectively, of the particle candidate in the central detector.

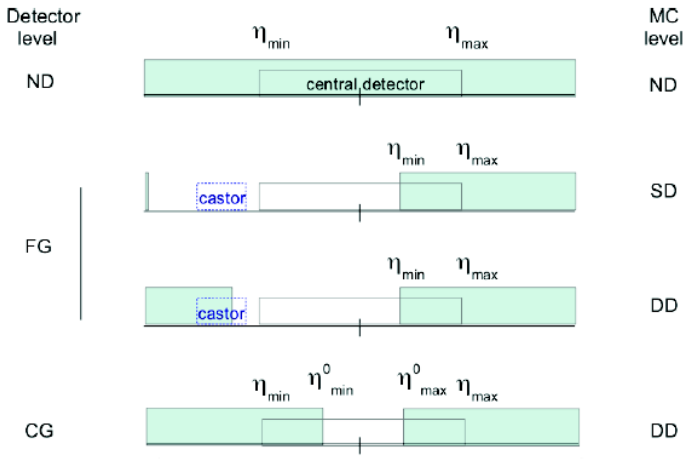

Figure 2: Event topologies in the final-state particle η space

In this analysis we do not show the Central Diffraction (CD) events separately, their contribution to the selected samples being negligible.

2 Forward rapidity gap cross section

In this event sample the forward rapidity gap cross sections are measured as a function of the fractional longitudinal momentum loss of the proton ξ_X, defined in terms of the mass of the dissociated system X, M_X, by the relation:

$$\xi_X = \frac{M_X^2}{s} \tag{1}$$

with s the center-of-mass energy squared.

The CASTOR calorimeter will allow to detect the hadronic system Y when it escapes the central detector. The activity (or lack of it) in CASTOR enables to distinguish (see figure 2) a SD event ($\log_{10}(M_Y/GeV) < 0.5$) from a DD event ($0.5 < \log_{10}(M_Y/GeV) < 1.1$). In the purely SD events, ξ_X represents the fractional longitudinal momentum loss of the scattered proton.

The differential cross sections measured in bins of ξ_X, separately for $\log_{10}(M_Y/GeV) < 0.5$ (no CASTOR tag) and $0.5 < \log_{10}(M_Y/GeV) < 1.1$ (CASTOR tag) are calculated using the formula:

$$\frac{d\sigma}{d\log_{10}\xi_X} = \frac{N^{evt}}{L \cdot (\log_{10}\xi_X)_{bin}} \tag{2}$$

where N^{evt} is the number of events in the bin, L is the integrated luminosity and $(\log_{10}\xi_X)_{bin}$ is the bin width.

We can see on figure 3 that when there is no activity in the CASTOR calorimeter, the cross section is dominated by SD events. Nevertheless we still have some contribution of DD events, which correspond to scattered systems escaping the detection in the CASTOR η region.

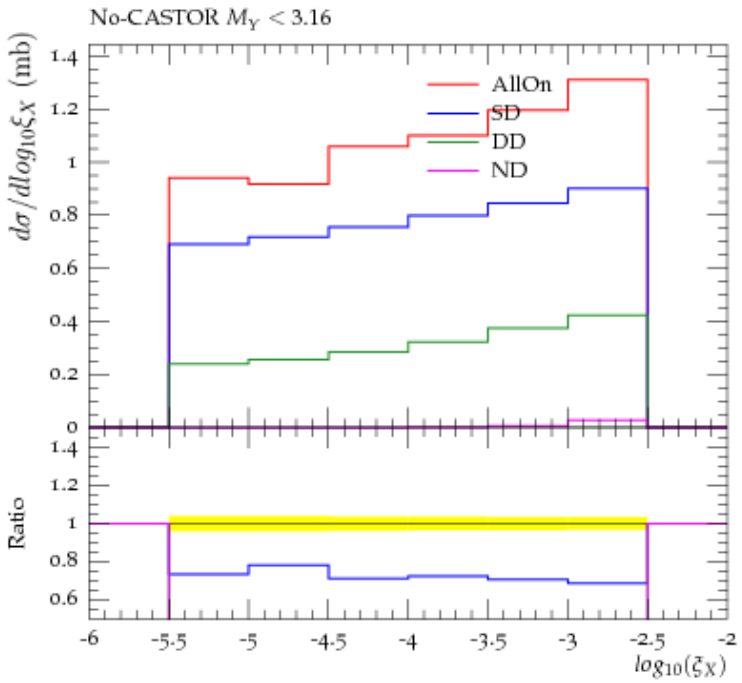

Figure 3: Contributions of the different diffractive processes to the FG sample without activity in CASTOR

On the other hand, when we have a LRG and activity in CASTOR, DD events will dominate the cross section, as shown on figure 4.

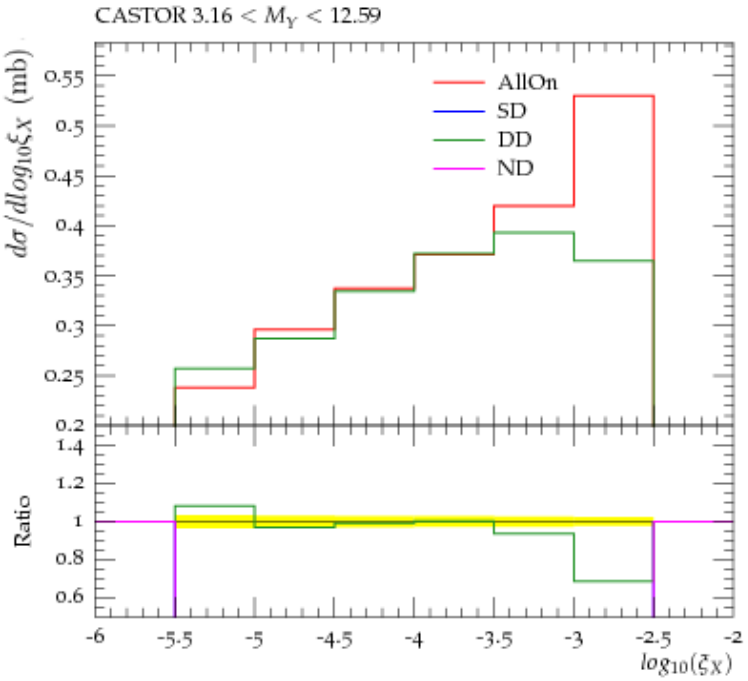

Figure 4: Contributions of the different diffractive processes to the FG sample when there is activity in CASTOR.

The following step is to focus on the different PYTHIA tunings and how they predict the behaviour of the cross sections for the different topologies. When there is no Y system in the CASTOR acceptance, the different tunings do not reproduce the data, as shown in figure 5. Most of them predict a cross section increasing with ξ_X. The MBR model is the only one that slightly decreases with ξ_X and the closest to the data.

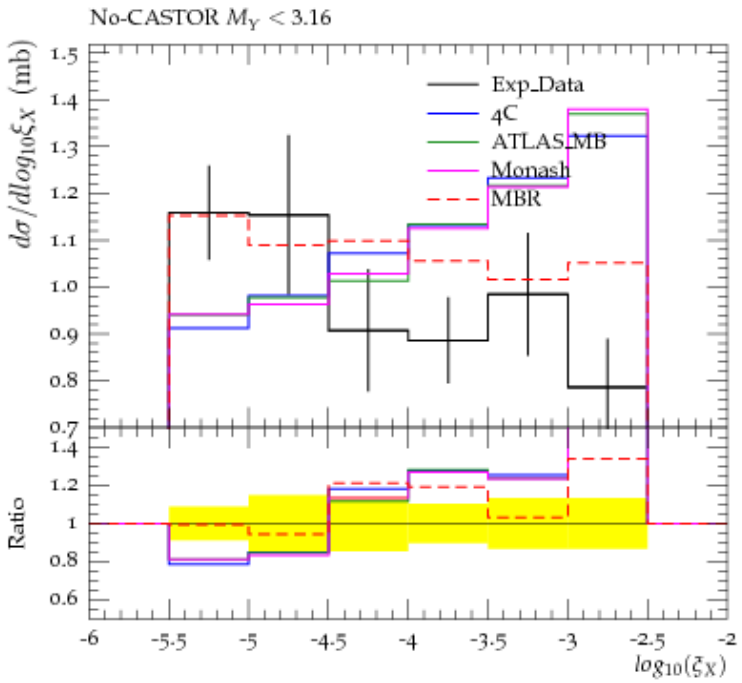

Figure 5: PYTHIA8 tuning predictions when there is no activity in CASTOR.

However, when we have activity in CASTOR (fig 6), the differential cross section is better explained by the PYTHIA8 Monash tuning for low ξ_X values, where the MBR model overestimates the data. Nevertheless, for higher values of ξ_X, where the dissociation mass is higher, the differential cross section is not well explained by any of the PYTHIA8 predictions.

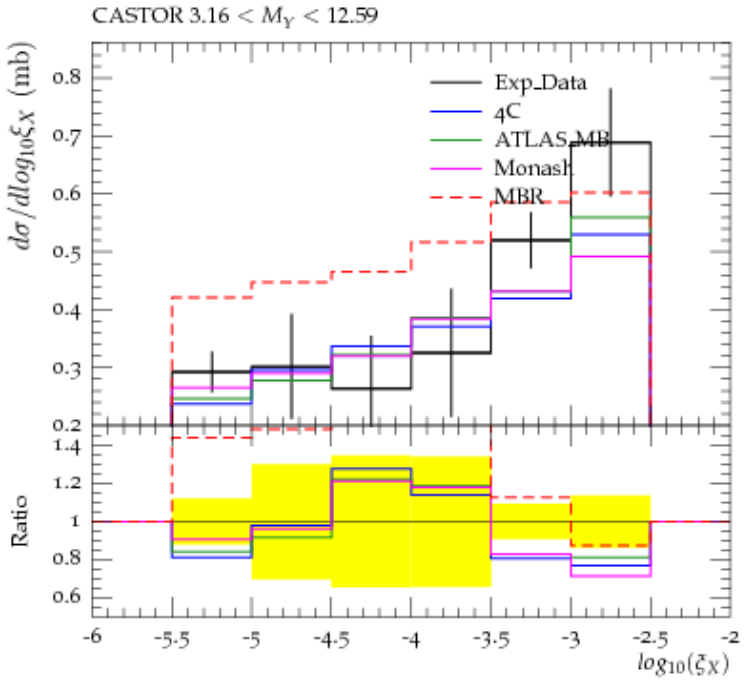

Figure 6: Different PYTHIA8 tuning predictions when there is activity in CASTOR.

3 Central rapidity gap cross section

The variable ξ is related to the masses of the diffractive dissociated systems by the relation:

$$\xi = \frac{M_X^2 \cdot M_Y^2}{s \cdot m_p^2}, \tag{3}$$

where M_X (M_Y) is the mass of the X (Y) system and m_p the proton mass. The size of the LRG, $\Delta\eta$, is related to ξ through $\Delta\eta = -\log\xi$. Following the definition for the cuts that are defined in [1] in order to reproduce the acceptance of the detector, we consider the differential cross section of the events that fulfil the conditions $\Delta\eta > 3$, $\log_{10}(M_X/GeV) > 1.1$ and $\log_{10}(M_Y/GeV) > 1.1$. The differential cross section will be calculated as

$$\frac{d\sigma}{d\Delta\eta} = \frac{N^{evt}}{L \cdot (\Delta\eta)_{bin}} \tag{4}$$

where N^{evt} is the number of events in the corresponding bin, L is the integrated luminosity and $(\Delta\eta)_{bin}$ is the bin width.

The PYTHIA8-4C predictions for the CG sample are compared to the CMS measurement on figure 7. The different contributions (SD, DD, ND) are also shown. As expected, one can see that the dominant contribution comes from Double Dissociation (DD) events and that the Non-Diffractive contribution is negligible.

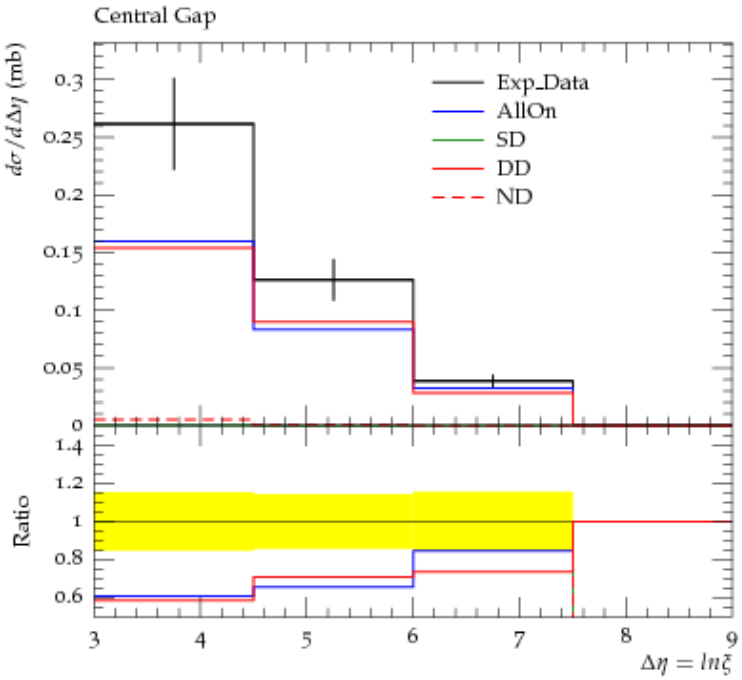

Figure 7: Comparison of the P8-4C predictions to the CMS measurement for the CG sample

The comparison of the measured differential cross section with the predictions of the models is shown in figure 8. The predictions of the MBR model give the best description of the data, while the different tunings of PYTHIA8 are not able to describe them.

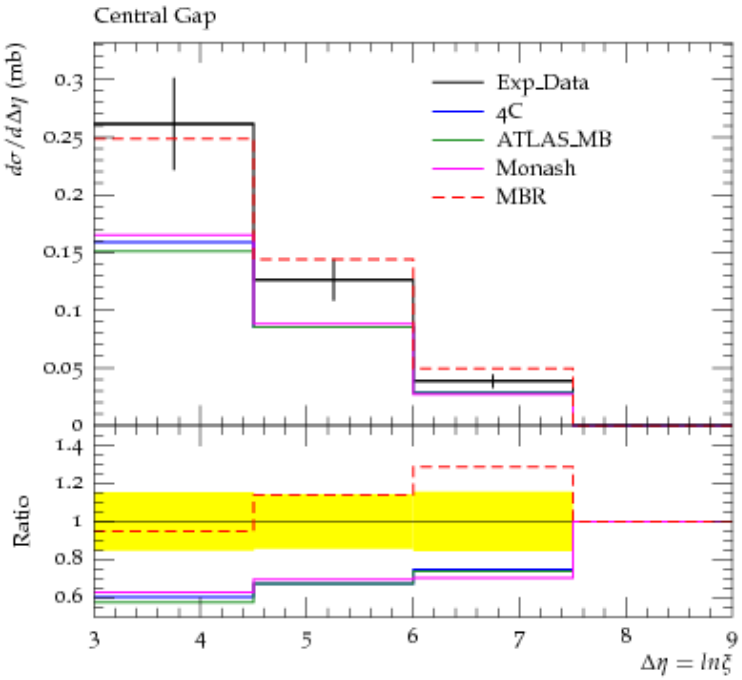

Figure 8: Different PYTHIA8 tuning predictions for the CG topology

4 Summary

The code made to determine the MC generator predictions and compare them with the data obtained in the 2010 commissioning period was implemented in RIVET. The code was validated with [1].

The cross section with no-CASTOR activity (σ_{noCAS}) is dominated by SD events, whilst the CG (σ_{CG}) and FG with CASTOR activity (σ_{CAS}) samples are mainly produced by DD events. We can also see that the ND contribution to these cross sections is negligible.

The main background to σ_{noCAS} is due to DD events. On the other hand, σ_{CAS} and σ_{CG} owe their dominating background from ND events, whereas the SD contribution is negligible.

The used PYTHIA8 configurations do not describe precisely the experimental data obtained in 2010 when there was low pileup and a new tuning is needed to predict these and further data.

5 Acknowledgments

I am very grateful to have received such patient and kind help from Hannes Jung's research group who made me realize the dynamics of a research group when working in this field of physics. Moreover, I would like to thank explicitly both Benoît and Hannes for the time they took to answer my questions throughout the development of this work.

I would also like to thank the Mexican Society of Physics' (SMF) Department of Particles and Fields (DPyC) for their unquestionable support, specially to Arturo Fernandez Tellez for his moral and economical support.

References

[1] R. Ciesielski, K. Goulianos, A.V. Pereira, S. Sen, T. Yetkin. "Measurement of diffractive dissociation cross sections in pp collisions at $\sqrt{s} = 7$ TeV" *CMS collaboration*. CMS Paper FSQ-12-005.

[2] T. Sjöstrand, S. Mrenna and P.Z. Skands, "A Brief Introduction to PYTHIA8.1", *Comput.Phys.Commun.* **178** (2008) 852, doi:10.1016/j.cpc.2008.01.036, arXiv¿071..3820.

[3] P. Skands, S. Carrazza, J. Rojo. "Tuning PYTHIA8.1: the Monash 2013 tune". arXiv:1404.5630

[4] R. Ciesielski and K.Goulianos, "MBR Monte Carlo Simulation in PYTHIA8", arXiv:1205.1446.